A new modified B4 inverter using SRF controller with SVPWM technique for grid-connected PV system

Golkonda Anitha[1], Krishnaveni Kondreddi[2], Guduri Yesuratnam[3]
[1]Department of Electrical Engineering, University College of Engineering, Osmania University, Hyderabad, India
[2]Department of Electrical and Electronics Engineering, Chaitanya Bharathi Institute of Technology, Hyderabad, India
[3]Department of Electrical Engineering, UCE, Osmania University, Hyderabad, India

Article Info

ABSTRACT

The integration of renewable power sources into the grid presents a complex challenge, as the grid operates at AC voltage, while photovoltaic (PV) arrays generate DC power. A 3-phase inverter synchronizes with the grid's voltage and frequency for efficient energy integration. In conventional technique, a 3-ph 6-switch (B6) inverter is used for sharing the power to the grid. In this paper reduced switch count 3-ph 4-switch (B4) inverter topology is introduced with reduced power losses. This topology has 4 insulated gate bipolar transistor (IGBT) switches and two capacitors replacing the other 2 switches positioned in one leg of the inverter, which connects to a grid-connected PV system. A grid synchronization method called synchronous reference frame (SRF) based proportional integral (PI) is used to track the phase angle of the grid and subsequently inject current into the grid. A B4 inverter is operated by a novel space vector pulse width modulation (SVPWM) control technique which operates in 4 possible switching states. A comparative analysis is carried out with the PV array grid integration connected through B4 and B6 inverter topologies with SRF control. The modeling and design are carried out in a MATLAB/Simulink environment with graphs plotted according to the conditions. The comparative analysis validates the importance of SRF controllers for the grid integration of any renewable source.

Corresponding Author:

Golkonda Anitha
Department of Electrical Engineering, University College of Engineering, Osmania University
Hyderabad, India
Email: mahanitha2006@gmail.com

1. INTRODUCTION

Renewable source penetration into the grid has become a mandatory requirement for load compensation using natural resources [1]. Renewable power is the only solution to the current day problem of global warming and climatic shift. Most of the power generation plants use fossil fuels like coal, diesel, and uranium, which create a carbon print on the planet. The fumes and discharge from these sources lead to climatic disasters creating unlivable conditions for the beings on the planet. It is high time to shift the power generation to renewable sources that have zero emissions. Sharing renewable power to the grid is a critical task as the natural sources (solar irradiation, winds) are unpredictable [2]. Of all the available renewable sources, solar power generation is considered to be the most flexible and easy to install.

Solar power generation involves photo voltaic panels connected in different combinations of parallel and series sets forming a photovoltaic array (PVA) [3]. The accumulated powers from each panel are considered to be the total power of the PVA. The PVA generates power in DC voltage which needs to be

converted to AC for sharing to the grid. The converters can either be 1-ph or 3-ph as per the availability of the grid. In most of the commercial and remote installations of the PVA plants the power is shared to a 3-ph grid [4]. The 3-ph grid interconnection of PVA needs a 3-ph voltage source inverter (VSI) which converts the DC voltage of PVA to two-level 3-ph AC voltages. The B4 inverter offers improved efficiency over the B6 inverter by reducing switching and conduction losses through fewer power switches. Still, it is important to consider the traditional 4-switch inverter's drawbacks including circulating unbalanced currents in the third phase of the inverter which is connected to the mid-point of a capacitor. In certain articles, the standard modulation techniques have been given additional limitations in an attempt to address the issue as mentioned above [5]. Wang *et al.* [6] discuss a new modulation scheme and the dc-link capacitor voltage fluctuation of the four-switch three-phase inverter in detail. Zhang *et al.* [7] which neutralizes the effect of capacitor voltage fluctuation and produces a balanced 3-phase L-L voltages. The space vector PWM technique for FSTPI under DC-link voltage imbalance or ripples has been proposed by Lee *et al.* [8] proposed a mathematical transformation for the development of basic space vectors and modulation techniques comparable to 6-switch 3-phase inverters. Blaabjerg *et al.* [9] determined that an adaptive space vector modulation (SVM) algorithm may reduce the DC-voltage ripple effect on the B4 inverter output, which has the benefit of enhancing the DC-link filter's response and raising the inverter's output quality. The conventional two-level voltage source converter (VSC) is a B6 topology with 3 legs included with two switches in each leg. For sharing the PVA power to the grid, synchronization of 3-ph voltages needs to be done where the voltage amplitude, frequency, and phase need to be matched. To achieve this synchronous reference frame (SRF) controller is integrated into the VSI [10]-[12]. The SRF controller operates by taking feedback from grid and inverter voltages and currents respectively.

The B6 VSC is a traditional circuit that has higher losses and creates more harmonics in the currents. In this paper, the conventional VSI is replaced by a 4-switch VSI called B4 inverter which has the same structure but with two capacitors replacing the insulated gate bipolar transistors (IGBTs) of one phase leg. The conventional PWM of the SRF controller is replaced with a novel space vector pulse width modulation (SVPWM) technique, which utilizes only 4 switching states [13]. The test system for the analysis includes a PVA connected to a 4-switch VSI operated by the SRF-SVPWM technique. The output of the inverter is connected to an LC filter for harmonics compensation and further connected to the grid. The complete test system for the analysis is given in Figure 1.
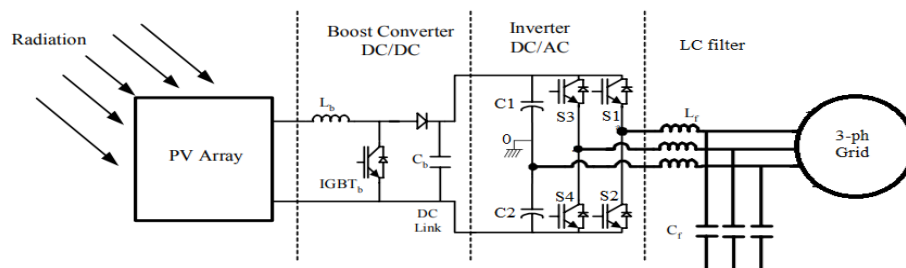

Figure 1. Proposed test system with PVA connected 4-switch VSI

As observed in Figure 1 the PVA is connected to the B4 VSI through a boost converter operated by perturb and observe (P&O) maximum power point tracking (MPPT) algorithm for maximum power extraction. At the output of the boost converter, the 4-switch VSI topology is connected [14]. As an alternative to the conventional 6-switch inverter, the 4-switch inverter offers several benefits: it requires fewer interface circuits to supply PWM signals to the switches, which lowers cost and increases reliability. It also reduces conduction and switching losses by one-third by eliminating one leg. This paper presents a novel adaptive SVPWM technique that was designed and optimized for B4 inverter topology, which significantly reduces balanced currents in the circuit and reduced total harmonic distortion (THD) when connected to the grid through a PVA.

This paper is organized into five sections, where section 1 has the introduction to the test system and the outline of the proposed techniques and topologies. The following section 2 has the configuration of the proposed PVA-connected 4-switch VSI topology. In section 3 the complete control structure design with SRF-SVPWM for controlling the 4-switch VSI is included. The modeling and results are shown in section 4 with a comparative analysis between 6-switch and 4-switch VSI topologies. The final section 5 of the paper is included with the conclusion to the paper defining and validating the better circuit module for the given application followed by references set in this paper.

2. PROPOSED METHOD

The PVA is designed with a specific combination of series and parallel panels to generate the required voltage for the VSI to inject power into the grid. To achieve maximum power extraction from the PVA and maintain a stable DC voltage, a boost converter is necessary. The boost converter is controlled by the P&O MPPT method, which is a fast and simple technique for controlling the converter [15]. The duty ratio of the boost converter switch is adjusted based on changes in PVA voltage and current determined by the MPPT technique. These values vary according to changes in solar irradiation. The following expressions determine the change in duty ratio (D) based on the PVA voltage and current.

$$D_n = D_{n-1} + \Delta D; \begin{Bmatrix} \text{If } P(n) > P(n-1) \text{ and } V(n) > V(n-1) \\ \text{If } P(n) < P(n-1) \text{and } V(n) < V(n-1) \end{Bmatrix} \tag{1}$$

$$D_n = D_{n-1} - \Delta D; \begin{Bmatrix} \text{If } P(n) > P(n-1) \text{ and } V(n) < V(n-1) \\ \text{If } P(n) < P(n-1) \text{and } V(n) > V(n-1) \end{Bmatrix} \tag{2}$$

Here, $V(n)$ $P(n)$ and D_n are the present values of voltage, power of PVA, and duty ratio of the circuit. $V(n-1)$ $P(n-1)$ and D_{n-1} are the previous values of voltage, power of PVA, and duty ratio of the circuit. The ΔD denotes the update to the duty ratio either increased or decreased concerning the conditions given in (1) and (2). After maximum power extraction of the PVA power, the boost converter is connected to a 4-switch VSI which converts the stabilized boosted DC voltage to 3-ph AC voltages [16]. The 4-switch inverter has unique topology and modulation requirements, necessitating the development of specialized modulation techniques. Among these advanced methods, SVM has emerged as a prominent solution, drawing attention for its simplicity and straightforward implementation. A comparative vector diagram illustrating the differences between 6-switch and 4-switch inverters is shown in Figure 2. The space vector diagram for a three-phase 6-switch inverter is shown in Figure 2(a) [17]. The SVPWM method involves creating a reference vector on a plane divided into four sectors (I-IV), where active vectors and their durations within a sampling interval are selected and calculated based on the required V_{ref} location in each sector, as depicted in Figure 2(b).

As per the given Figure 2 the 6-sector phasor is converted to a 4-sector phasor as per the V_{ref} angle determined by the grid voltage waveform. Each sector has a specific switching sequence for the switches of the 4-switch VSI [18]. The switching sequence for each sector as per the V_{ref} angle can be observed in Table 1.

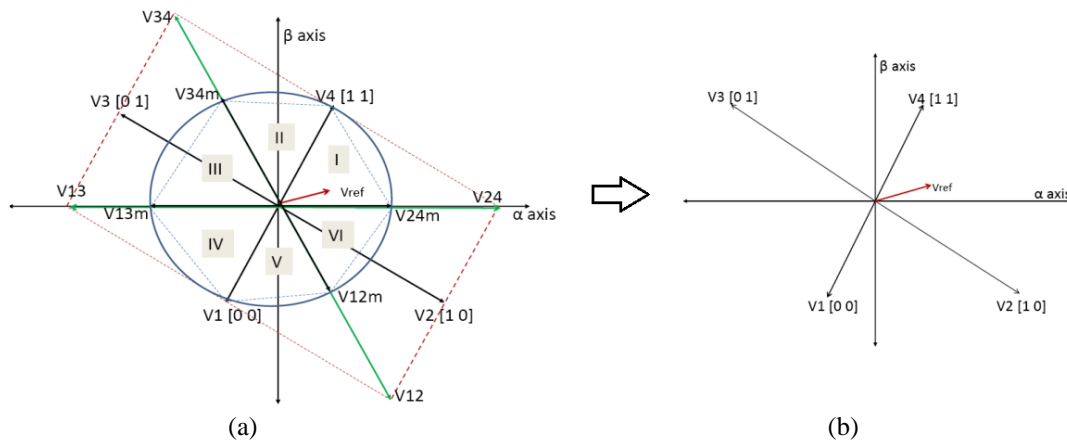(a)   (b)

Figure 2. Vector diagram of (a) comparison of 6-switch and 4-switch VSI and
(b) 4-switch VSI with four vectors

Table 1. Switching sequence for 4-switch VSI

V_{ref} angle	V_{an}	V_{bn}	V_{cn}	V_{ab}	V_{bc}	V_{ca}	V_α	V_β	V_i	S_1	S_2	S_3	S_4
-120	-Vdc/3	-Vdc/3	+2Vdc/3	0	-Vdc	+Vdc	+Vdc/3	$-Vdc/\sqrt{3}$	2Vdc/3	0	1	0	1
-30	+Vdc	-Vdc	0	+2Vdc	-Vdc	-Vdc	-Vdc	$-Vdc/\sqrt{3}$	$2Vdc/\sqrt{3}$	1	0	0	1
60	+Vdc/3	+Vdc/3	-2Vdc/3	0	+Vdc	-Vdc	+Vdc/3	$+Vdc/\sqrt{3}$	2Vdc/3	1	0	1	0
150	-Vdc	+Vdc	0	-2Vdc	+Vdc	+Vdc	-Vdc	$+Vdc/\sqrt{3}$	$2Vdc/\sqrt{3}$	0	1	1	0

As per the given table, the voltages of the inverter are expressed as (3).

$$V_{ab} = V_{an} - V_{bn}; V_{bc} = V_{bn} - V_{cn}; V_{ca} = V_{cn} - V_{an} \qquad (3)$$

Here, $V_{ao}V_{bo}V_{co}$ are the phase voltages with respect to point '0' in the 4-switch VSI. The point '0' is the grounded point between the two capacitors C1 and C2 [19], [20]. Concerning the input voltage V_{dc} to the inverter, the voltages are expressed as (4).

$$V_{ao} = (2S_1 - 1)\frac{V_{dc}}{2}; V_{bo} = (2S_3 - 1)\frac{V_{dc}}{2}; V_{co} = 0; \qquad (4)$$

The phase-to-ground voltages are expressed as (5).

$$V_{an} = (4S_1 - 2S_3 - 1)\frac{V_{dc}}{3}; V_{bn} = (4S_3 - 2S_1 - 1)\frac{V_{dc}}{3}; V_{cn} = (1 - S_1 + S_3)\frac{2V_{dc}}{3} \qquad (5)$$

The space vector resultant signal from the phase voltages of the inverter is determined by the following expressions as (6).

$$V_i = \frac{2}{3}(V_{an} + aV_{bn} + a^2V_{cn}) \qquad (6)$$

From the phase to ground voltages the αβ voltage components are determined using Clark's transformation expressions as (7).

$$V_\alpha = \frac{2}{3}(V_{an} - 0.5V_{bn} - 0.5V_{cn}); V_\beta = \frac{1}{\sqrt{3}}(V_{bn} - V_{cn}) \qquad (7)$$

From the given equations the new vectors formed for the 4-switch VSI based on 6-switch VSI vectors as per Figure 2 are expressed as (8).

$$V_{24m} = \frac{1}{2}V_{24}; V_{34m} = \frac{1}{2}V_{34}; V_{13m} = \frac{1}{2}V_{13}$$
$$V_{12m} = \frac{1}{2}V_{12}; V_{0m} = \frac{1}{2}(V_1 + V_4) \qquad (8)$$

The vector comparison of the 4-switch VSI and 6-switch VSI are given in Table 2. As per Table 2, the 6 vectors of the 6-switch VSI are replaced by the 6-vectors of the 4-switch VSI creating 3-ph AC voltages for the grid integration [21]. For synchronization of the 4-switch VSI to the grid the V_{ref} voltage signal is generated by SRF controller taking feedback from grid voltages and inverter currents.

Table 2. Vectors comparison of 4-switch VSI and 6-switch VSI

4-switch VSI	6-switch VSI
V_{24m}	V_1
V_4	V_2
V_{34m}	V_3
V_{13m}	V_4
V_1	V_5
V_{12m}	V_6

3. DESIGN OF SRF CONTROLLER

The SRF controller is considered to be the finest control module for the integration of renewable sources into the grid. The SRF control structure is very simple and has a less complex mathematical model which helps the controller with faster response [22]. The SRF controller is generally used for generating reference voltages to any PWM technique controlling the VSI. The Sin reference signals from the SRF controller ensure grid synchronized operation of the VSI. The SRF controller takes feedback from the grid phase voltages and VSI currents (in per unit representation) and calculates the reference signals [23], [24]. The complete structure of the SRF controller can be observed in Figure 3.
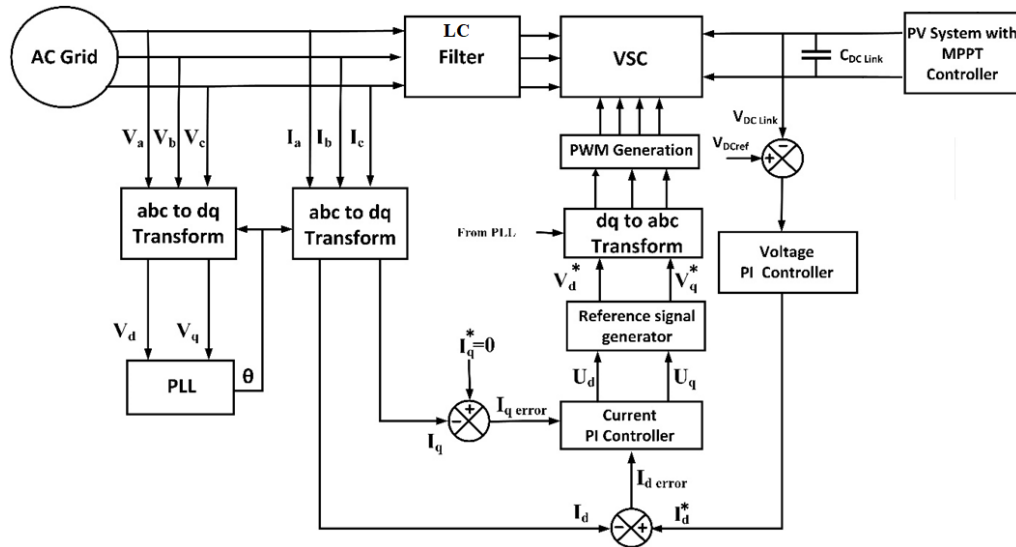
Figure 3. SRF control structure with grid and inverter feedback

The magnitude, frequency, and phase of the VSI output voltages are controlled by the SRF reference signals making it follow the grid [25]. For generating the Sine reference signals the complete controller is designed in dq component format using Park's transformation as (9).

$$\begin{bmatrix} F_d \\ F_q \end{bmatrix} = \frac{2}{3} \begin{bmatrix} \text{Sin wt} & \text{Sin}\left(\text{wt} - \frac{2\pi}{3}\right) & \text{Sin}\left(\text{wt} + \frac{2\pi}{3}\right) \\ \text{Cos wt} & \text{Cos}\left(\text{wt} - \frac{2\pi}{3}\right) & \text{Cos}\left(\text{wt} + \frac{2\pi}{3}\right) \end{bmatrix} \begin{bmatrix} F_a \\ F_b \\ F_c \end{bmatrix} \tag{9}$$

In the given expression (9), 'F' represents any signal either voltage 'V' or current 'I'. 'wt' is the phase angle of the grid voltage of phase 'A' determined by phase lock loop (PLL) [26], [27]. The voltage dq components for the generation of reference signals are expressed as:

$$\vartheta_d^* = Ud + \vartheta d + L\omega i_q \tag{10}$$

$$\vartheta_q^* = Uq + \vartheta q - L\omega i_d \tag{11}$$

here, $\vartheta d \ \vartheta q$ and $i_d i_q$ are determined by (9) which are the grid voltages and inverter currents dq components. The Ud and Uq components are determined by the current controller (PI controller) with input taken from error dq current components as expressed as:

$$Ud = (i_{d\,ref} - i_d)\left(K_{pi} + \frac{K_{ii}}{s}\right) \tag{12}$$

$$Uq = \left(i_{q\,ref} - i_q\right)\left(K_{pi} + \frac{K_{ii}}{s}\right) \tag{13}$$

here, $i_{d\,ref} \ i_{q\,ref}$ are the reference dq current components. $K_{pi} \ K_{ii}$ the proportional and integral gains of the current controller are determined by the trial-and-error method. The $i_{q\,ref}$ is considered to be zero and the $i_{d\,ref}$ is expressed as:

$$i_{d\,ref} = (\vartheta_{dc\,ref} - \vartheta_{dc})\left(K_{pv} + \frac{K_{iv}}{s}\right) \tag{14}$$

here, $\vartheta_{dc\,ref}$ is the reference DC link voltage input to the 4-switch VSI. $K_{pv} \ K_{iv}$ are the proportional and integral gains of the voltage controller tuned as per the response of the controller [28]. The reference signals generated by the expressions (10) and (11) are converted to Sine signals using inverse Park's expressions given as:

$$\begin{bmatrix} \vartheta_a \\ \vartheta_b \\ \vartheta_c \end{bmatrix} = \begin{bmatrix} \text{Sin wt} & \text{Cos wt} \\ \text{Sin}\left(wt - \frac{2\pi}{3}\right) & \text{Cos}\left(wt - \frac{2\pi}{3}\right) \\ \text{Sin}\left(wt + \frac{2\pi}{3}\right) & \text{Cos}\left(wt + \frac{2\pi}{3}\right) \end{bmatrix} \begin{bmatrix} \vartheta_d \\ \vartheta_q \end{bmatrix} \tag{15}$$

the final reference signals ϑ_a ϑ_b ϑ_c are given input to the 4-switch VSI controller to determine the V_{ref} signal for the generation of pulses to the 4 switches.

4. RESULTS AND DISCUSSION

With the given structure and design of the test system and control modules as per Figures 1 to 3 the modeling is done in MATLAB/Simulink tool. All the blocks for the modeling are considered from the 'Electrical' blocks of the Simulink library. Figure 4 indicates the MATLAB/Simulink diagram of the 4-switch VSI-connected PVA grid interconnection. The parameters for the modeling are considered from the configuration as shown in Table 3.

These parameters from Table 3 are considered for the test system and the simulation is carried out for both 6-switch and 4-switch VSI. The results generated are plotted in graphical representation and compared. The simulation is run for 2sec and plots for PV parameters, inverter power, AC side 3-ph voltages, and currents are considered with respect to time.
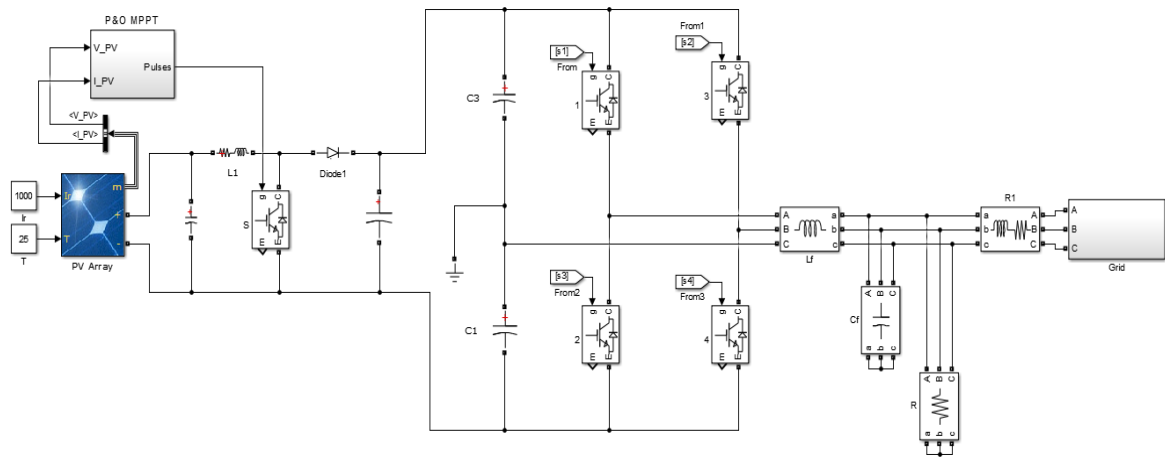

Figure 4. 4-switch VSI connected PVA grid interconnection

Table 3. Configuration parameters

Name of the module	Parameters
PVA	V_{mp} = 54.7 V, I_{mp} = 5.58 A, V_{oc} = 64.2 V, I_{sc} = 5.96 A, N_s = 5, N_p = 3, P_{pva} = 4.5 kW.
Boost converter	L_{boost} = 1 mH, C_{in} = 100 μF, C_{out} = 12 mF, R_{igbt} = 0.1 Ω, R_{diode} = 0.01 Ω.
Inverter	R_{igbt} = 0.1 Ω, C_1 = C_2 = 1000 μF, L_f = 1 mH, C_f = 100 μF.
Grid	440 Vrms, 50 Hz, R_g = 0.1 Ω, L_g = 0.1 mH.
Load	Rload = 100 Ω.
SRF SVPWM	Vdcref = 400 V, Kpv = 0.05, Kiv = 0.002, Kpi = 0.005, Kii = 0.0035.

Figure 5 illustrates the SRF controller modeling with input from grid voltages, inverter currents, and DC link voltage. The SRF controller voltage and current controllers (PI) are tuned as per the response of the inverter. The complete structure is modeled in per unit representation for faster response of the system.
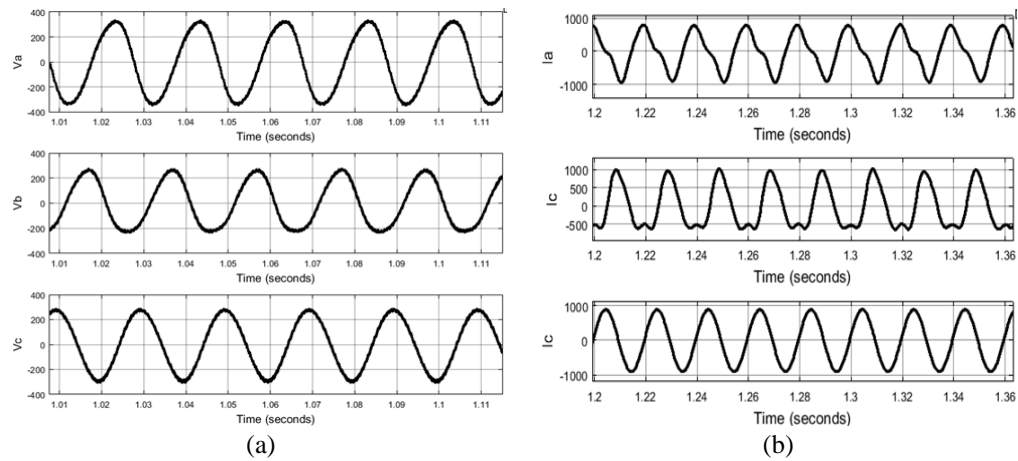
Figure 5. SRF controller modeling

Figure 6 shows the power of the PVA extracted by the boost converter is recorded at 4 kW. This power needs to be delivered to the grid at a higher voltage of 400 V as seen in Figure 7. The DC link voltage oscillates between 300 V and 400 V as the VSI is connected to the grid which creates circuiting currents in the inverter increasing the ripple of DC voltage. Figure 8 shows the output simulation results of the 3-ph 4-switch inverter. Figure 8(a) shows the 3-ph voltages and Figure 8(b) indicates the 3-ph currents of the 4-switch VSI. Due to the conventional PI controller, the ripple in the voltage is higher creating harmonics in the inverter currents. However, the voltage harmonics of the inverter are less as compared to the currents. The injected active and reactive powers of the inverter are shown in Figure 9 with 3.5 kW and 1.2 kVAR shared to the grid. Figure 10 represents the power loss calculated by the comparison of PVA power and power delivered by the inverter.

As observed in Figure 10 the power loss of the 6-switch VSI is 1,500 W and the 4-switch VSI is 500 W. Comparatively, the 4-switch inverter delivers an extra 1,000 W for the same rating of the PVA and the grid. The inverter voltages are analyzed using the Fast Fourier Transform (FFT) analysis tool to determine the THD of the signal and are presented in Figure 11. Figure 11(a) shows the THD of the 6-switch inverter and Figure 11(b) shows the THD of the 4-switch inverters. Harmonics of both the VSIs are noted to be 1.98% and 1.7% for 6-switch and 4-switch inverters respectively. The analysis of voltages is carried out at the same time with the same rating of the system and PVA.

Figure 6. DC link voltage input 4-switch VSI

Figure 7. P_pv extracted power

Figure 8. Output simulation results of the 3-ph 4-switch inverter for (a) 3-ph voltages of the 4-switch VSI and (b) 3-ph current of the 4-switch VSI
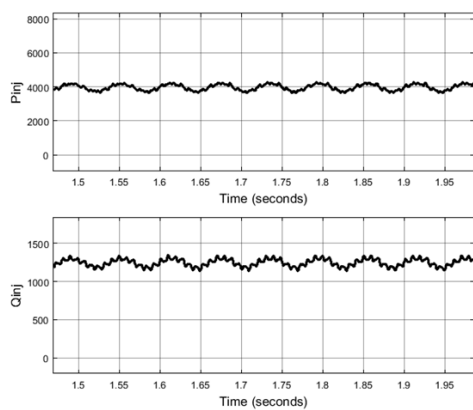

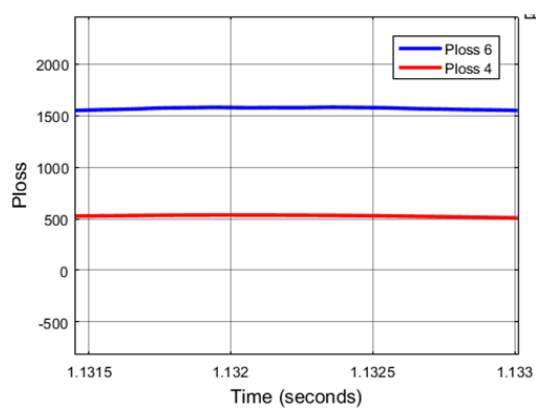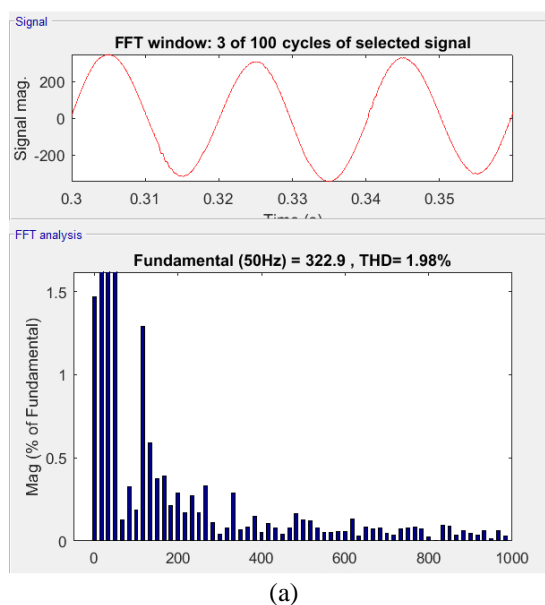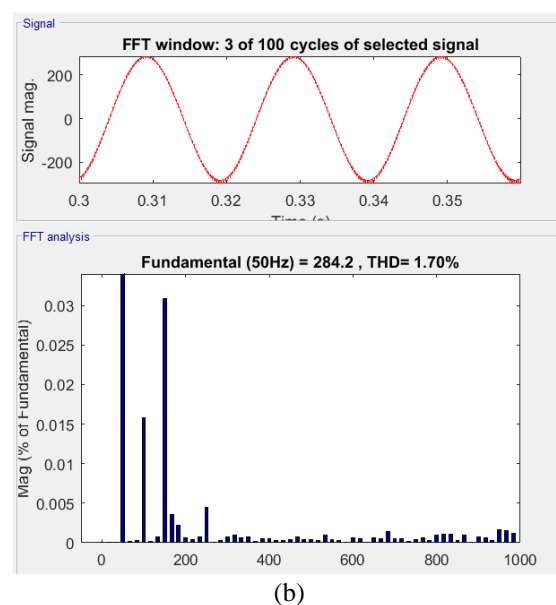Figure 9. Active and reactive powers injected to the grid

Figure 10. Power loss comparison of 6-switch and 4-s

Figure 11. THD analysis of (a) 6-switch and (b) 4-switch VSI voltage with FFT tool

The results show that by employing the SRF controller and SVPWM technique, the output voltage of the B4 inverter is remarkably close to that of the B6 inverter. This indicates that the B4 inverter, despite having fewer switches, can achieve comparable performance to the B6 inverter, making it a promising option for grid-connected PV applications.

5. CONCLUSION

This paper presents a comprehensive test system for grid-connected PV applications, utilizing B4 and B6 inverter topologies with synchronization controllers. The study encompasses the design and modeling of a 4-switch inverter, including a detailed mathematical model of its switching states. An SRF controller is employed to generate reference signals for the 4-switch SVPWM inverter to achieve synchronization. Furthermore, a comparative analysis is conducted between the 4-switch and 6-switch inverter configurations for the same PVA system rating, providing valuable insights into their performance and efficiency. The 6-switch VSI delivers 3 kW power, while the 4-switch VSI delivers 4 kW power. The 6-switch VSI has an extra power loss of 1,000 W due to its conventional SVPWM and extra switches. The harmonic distortion of the 6-switch VSI is calculated to be 1.98%, while the 4-switch VSI has a comparatively low harmonic distortion of 1.7%. Therefore, the 4-switch VSI has better performance than the 6-switch VSI, as it is more efficient and has fewer harmonics. The 4-switch VSI topology operates with very low power loss when adopted in higher rating systems. The performance of the proposed topology can be further improved by updating the controllers.

AUTHOR CONTRIBUTIONS STATEMENT

Name of Author	C	M	So	Va	Fo	I	R	D	O	E	Vi	Su	P	Fu
Golkonda Anitha		✓	✓		✓	✓		✓	✓					
Krishnaveni Kondreddi	✓	✓			✓	✓	✓	✓	✓		✓	✓	✓	✓
Guduri Yesuratnam	✓	✓			✓	✓	✓	✓	✓		✓	✓	✓	✓

C : **C**onceptualization	I : **I**nvestigation	Vi : **Vi**sualization
M : **M**ethodology	R : **R**esources	Su : **Su**pervision
So : **So**ftware	D : **D**ata Curation	P : **P**roject administration
Va : **Va**lidation	O : Writing - **O**riginal Draft	Fu : **Fu**nding acquisition
Fo : **Fo**rmal analysis	E : Writing - Review & **E**diting	

CONFLICT OF INTEREST STATEMENT

No conflict of interest.

DATA AVAILABILITY

- The data that support the findings of this study are openly available in [W. Wang, A. Luo, X. Xu, L. Fang, T. M. Chau, and Z. Li] at 10.1049/iet-pel.2012.0391, [5].
- The data that support the findings of this study are openly available in [R. Wang, J. Zhao, and Y. Liu] at 10.1109/IECON.2011.6119492, [6].
- The data that support the findings of this study are openly available in [H. H. Lee, P. Q. Dzung, L. D. Khoa, L. M. Phuong, and H. T. Thanh] at 10.1109/TENCON.2008.4766516, [8].

- The data that support the findings of this study are openly available in [K. S. Fuad, E. Hossain, and M. R. U. Chowdhury] at 10.1109/ICISET.2016.7856524, [10].
- The data that support the findings of this study are openly available in [S. Chatterjee and S. Chatterjee] at 10.1109/ICPDEN.2015.7084493, [11].
- The data that support the findings of this study are openly available in [H. Zhang] [10.1109/GreenTech56823.2023.10173831], [7].
- The data that support the findings of this study will be available in [S. Golestan, J. M. Guerrero, and J. C. Vasquez S.] at [10.1109/TPEL.2017.2719285], [27]
- The data that support the findings of this study are openly available in [in Y. P. Bhatt and M. C. Shah] at 10.1109/ICPEICES.2016.7853618, [24].
- The data that support the findings of this study are openly available in [A. H. Chander and L. Kumar] at 10.1109/INDICON.2017.8487990, [23].
- The data that support the findings of this study are openly available in [H. H. Lee, P. Q. Dzung, L. D. Khoa, L. M. Phuong, and H. T. Thanh] at 10.1109/TENCON.2008.4766516, [8].

REFERENCES

[1] P. Roy, J. He, T. Zhao, and Y. V. Singh, "Recent advances of wind-solar hybrid renewable energy systems for power generation: a review," *IEEE Open Journal of the Industrial Electronics Society*, vol. 3, pp. 81–104, 2022, doi: 10.1109/OJIES.2022.3144093.

[2] S. P. Bihari *et al.*, "A comprehensive review of microgrid control mechanism and impact assessment for hybrid renewable energy integration," *IEEE Access*, vol. 9, pp. 88942–88958, 2021, doi: 10.1109/ACCESS.2021.3090266.

[3] M. Shafiullah, S. D. Ahmed, and F. A. Al-Sulaiman, "Grid integration challenges and solution strategies for solar PV systems: a review," *IEEE Access*, vol. 10, pp. 52233–52257, 2022, doi: 10.1109/ACCESS.2022.3174555.

[4] K. N. Nwaigwe, P. Mutabilwa, and E. Dintwa, "An overview of solar power (PV systems) integration into electricity grids," *Materials Science for Energy Technologies*, vol. 2, no. 3, pp. 629–633, Dec. 2019, doi: 10.1016/j.mset.2019.07.002.

[5] W. Wang, A. Luo, X. Xu, L. Fang, T. M. Chau, and Z. Li, "Space vector pulse-width modulation algorithm and DC-side voltage control strategy of three-phase four-switch active power filters," *IET Power Electronics*, vol. 6, no. 1, pp. 125–135, 2013, doi: 10.1049/iet-pel.2012.0391.

[6] R. Wang, J. Zhao, and Y. Liu, "DC-link capacitor voltage fluctuation analysis of four-switch three-phase inverter," in *IECON Proceedings (Industrial Electronics Conference)*, 2011, pp. 1276–1281, doi: 10.1109/IECON.2011.6119492.

[7] H. Zhang, "Imbalance compensation for SVPWM-controlled four-switch three-phase inverters," in *2023 IEEE Green Technologies Conference (GreenTech)*, Apr. 2023, pp. 95–100, doi: 10.1109/GreenTech56823.2023.10173831.

[8] H. H. Lee, P. Q. Dzung, L. D. Khoa, L. M. Phuong, and H. T. Thanh, "The adaptive space vector PWM for four switch three phase inverter fed induction motor with DC - link voltage imbalance," in *TENCON 2008 - 2008 IEEE Region 10 Conference*, Nov. 2008, pp. 1–6, doi: 10.1109/TENCON.2008.4766516.

[9] F. Blaabjerg, D. O. Neacsu, and J. K. Pedersen, "Adaptive SVM to compensate DC-link voltage ripple for four-switch three-phase voltage-source inverters," *IEEE Transactions on Power Electronics*, vol. 14, no. 4, pp. 743–752, Jul. 1999, doi: 10.1109/63.774214.

[10] K. S. Fuad, E. Hossain, and M. R. U. Chowdhury, "Grid-voltage synchronization algorithm for grid tied renewable energy sources during adverse grid fault condition," in *2016 International Conference on Innovations in Science, Engineering and Technology (ICISET)*, Oct. 2016, pp. 1–5, doi: 10.1109/ICISET.2016.7856524.

[11] S. Chatterjee and S. Chatterjee, "Simulation of synchronous reference frame PLL based grid connected inverter for photovoltaic application," in *2015 1st Conference on Power, Dielectric and Energy Management at NERIST (ICPDEN)*, Jan. 2015, pp. 1–6, doi: 10.1109/ICPDEN.2015.7084493.

[12] X. Quan and A. Q. Huang, "PI-based synchronous reference frame frequency-locked loop," *IEEE Transactions on Industrial Electronics*, vol. 68, no. 5, pp. 4547–4553, May 2021, doi: 10.1109/TIE.2020.2985002.

[13] P. Gawhade and A. Ojha, "Recent advances in synchronization techniques for grid-tied PV system: a review," *Energy Reports*, vol. 7, pp. 6581–6599, Nov. 2021, doi: 10.1016/j.egyr.2021.09.006.

[14] M. G. Molina, "Modelling and control of grid-connected solar photovoltaic systems," in *Renewable Energy - Utilisation and System Integration*, InTech, 2016.

[15] D. Sera, L. Mathe, T. Kerekes, S. V. Spataru, and R. Teodorescu, "On the perturb-and-observe and incremental conductance MPPT methods for PV systems," *IEEE Journal of Photovoltaics*, vol. 3, no. 3, pp. 1070–1078, 2013, doi: 10.1109/JPHOTOV.2013.2261118.

[16] S. Saravanan and N. R. Babu, "Maximum power point tracking algorithms for photovoltaic system - a review," *Renewable and Sustainable Energy Reviews*, vol. 57, pp. 192–204, 2016, doi: 10.1016/j.rser.2015.12.105.

[17] A. A. Apte and V. D. Malwade, "Simulation of a 4-switch,3-phase inverter fed induction motor (IM) drive system," *International Journal of Innovations in Engineering Research and Technology [IJIERT]*, vol. 2, no. 2, 2015.

[18] G. Sowilam, "Six-space vector pulse width modulation of four-switch voltage source inverter feeding three phase induction motor," *ResearchGate*, 2015, doi: 10.13140/RG.2.1.3864.7522.

[19] F. Hicham, D. Yousfi, E. Mohamed Larbi, and A. Youness, "Four-switch three-phase PMSM converter with output voltage balance and DC-link voltage offset suppression," *Information*, vol. 8, no. 1, p. 11, Jan. 2017, doi: 10.3390/info8010011.

[20] K. K. Prabhakaran, A. Karthikeyan, S. Varsha, B. V. Perumal, and S. Mishra, "Standalone single stage PV-fed reduced switch inverter based PMSM for water pumping application," *IEEE Transactions on Industry Applications*, vol. 56, no. 6, pp. 6526–6535, Nov. 2020, doi: 10.1109/TIA.2020.3023870.

[21] U. Bose, K. Divya, V. Jyothi, and Sreejith S., "Performance analysis of four-switch three-phase inverter-fed induction motor drive," in *2014 Power and Energy Systems: Towards Sustainable Energy*, Mar. 2014, pp. 1–6, doi: 10.1109/PESTSE.2014.6805315.

[22] S. Masri, H. Aphieez, and J. K. R. Susila, "Modelling and performance analysis of synchronous reference frame phase-locked loop for three-phase grid-connected PV generation system," *Journal of Physics: Conference Series*, vol. 1764, no. 1, p. 012169, Feb. 2021, doi: 10.1088/1742-6596/1764/1/012169.

[23] A. H. Chander and L. Kumar, "Design of a synchronous reference frame controller for single phase standalone photovoltaic inverter," in *2017 14th IEEE India Council International Conference (INDICON)*, Dec. 2017, pp. 1–6, doi: 10.1109/INDICON.2017.8487990.

[24] Y. P. Bhatt and M. C. Shah, "Design, analysis and simulation of synchronous reference frame based Phase Lock Loop for grid connected inverter," in *2016 IEEE 1st International Conference on Power Electronics, Intelligent Control and Energy Systems (ICPEICES)*, Jul. 2016, pp. 1–5, doi: 10.1109/ICPEICES.2016.7853618.

[25] B. Aldbaiat, M. Nour, E. Radwan, and E. Awada, "Grid-connected PV system with reactive power management and an optimized SRF-PLL using genetic algorithm," *Energies*, vol. 15, no. 6, 2022, doi: 10.3390/en15062177.

[26] I. D. L. Costa, D. I. Brandao, L. M. Junior, M. G. Simões, and L. M. F. Morais, "Analysis of stationary- and synchronous-reference frames for three-phase three-wire grid-connected converter AC current regulators," *Energies*, vol. 14, no. 24, p. 8348, Dec. 2021, doi: 10.3390/en14248348.

[27] S. Golestan, J. M. Guerrero, and J. C. Vasquez, "A PLL-based controller for three-phase grid-connected power converters," *IEEE Transactions on Power Electronics*, vol. 33, no. 2, pp. 911–916, Feb. 2018, doi: 10.1109/TPEL.2017.2719285.

[28] M. Karimi-Ghartemani, "Synchronous reference frame PLL," in *Enhanced Phase-Locked Loop Structures for Power and Energy Applications*, Wiley, 2014, pp. 133–145.

BIOGRAPHIES OF AUTHORS

Golkonda Anitha received her B.Tech. in electrical and electronics engineering from the JNTU, Hyderabad in 2004 and M.Tech. from JNTU, Hyderabad in power electronics in 2011. She is currently a Ph.D. student at Osmania University, Hyderabad. Her research interests include renewable energy sources of power converters modulation techniques and power electronics. She can be contacted at email: mahanitha2006@gmail.com.

Krishnaveni Kondreddi completed her B.Tech. from Nagarjuna University in1992, M.S (DLPD) from BITS, Pilani in 1996, and M.Tech. from JNTU, Hyderabad, India in 2002. She is awarded a Ph.D. in electrical engineering in the area of flexible AC transmission systems from JNTU, Hyderabad in April 2009. Currently, she is working as a professor in the EEE Department of CBIT (A), Hyderabad. Her research interests include power electronics, FACTS, and applications of power electronics to renewable energy systems. She can be contacted at email: krishnaveni_eee@cbit.ac.in.

Guduri Yesuratnam completed his B.Tech. from JNTU, Hyderabad in 1995 and M.Tech. in power systems engineering, Regional Engineering College, Warangal in 1997. He was awarded a Ph.D. in electrical engineering from the Indian Institute of Science, Bangalore in 2007. Currently, he is working as a Sr. professor in the Department of Electrical Engineering, at Osmania University, Hyderabad. His research interests include computer aided power system analysis, reactive power optimization, power system security, voltage stability, AI applications in power systems, and gas insulated substations. He is serving as a peer reviewer of international journals. Throughout his career, he has supervised Ph.D. students as well as published many papers in IEEE as well as international conference proceedings and journals. He can be contacted at email: ratnamgy2003@gmail.com.